A relation between billiard geometry and the temperature of its eigenvalue gas

1997 J. Phys. A: Math. Gen. 30 129

(http://iopscience.iop.org/0305-4470/30/1/010)

J. Phys. A: Math. Gen. **30** (1997) 129–141. Printed in the UK PII: S0305-4470(97)71191-0

A relation between billiard geometry and the temperature of its eigenvalue gas

Hans-Jürgen Stöckmann, Ulrich Stoffregen and Michael Kollmann†
Fachbereich Physik, Universität Marburg, D-35032 Marburg, Germany

Received 18 January 1996, in final form 18 June 1996

Abstract. According to a conjecture of Yukawa the parametric motion of the eigenvalues of a chaotic system leads to a phase-space distribution proportional to $\exp(-\beta E)$ where E is the energy of the eigenvalue gas and β is its reciprocal temperature. To test the conjecture, in a first-step correspondence between the well known Pechukas–Yukawa level dynamics and that of a billiard with variable length is established. Next, β is expressed in terms of the billiard geometry thus fixing the only free parameter of the model. Finally, experimental distributions of eigenvalue velocities, curvatures etc, obtained from Sinai microwave billiards are analysed in terms of the model. In all cases a quantitative agreement was found, apart from some small deviations caused by the dominating bouncing-ball orbit.

1. Introduction

There is a close analogy between the level dynamics of a quantum system under the change of a parameter and the classical dynamics of a one-dimensional gas with a repulsive interaction potential. In this picture the eigenenergies take the role of the positions of particles and the parameter that of a time t. Pechukas [1] proposed a Hamiltonian with a linear parameter dependence,

$$\mathcal{H}(t) = \mathcal{H}_0 + Vt \tag{1}$$

and derived a dynamic equation system with eigenenergies x_n and matrix elements V_{nm} as dynamical variables. The ideas of Pechukas were developed further by Yukawa [2] who introduced eigenenergies x_n, their velocities $\dot{x}_n = V_{nn}$, and the interaction strengths $f_{nm} = |x_n - x_m|V_{nm}$ as variables, where the flow in phase space disappears under steady-state conditions. Yukawa conjectured that in analogy to statistical mechanics the stationary phase-space distribution should be given by

$$\rho \sim \exp\left(-\sum_i \beta_i C_i\right) \tag{2}$$

where the sum is over all constants of motion C_i, and β_i are the corresponding Lagrange parameters. The only constants of motion depending linearly or quadratically on $\dot{x}_n$ and f_{nm} are [3] the total momentum

$$P = \sum_n \dot{x}_n \tag{3}$$

† Present adress: ITF, UvA, Valckenstraat 65, 1018 XE Amsterdam, the Netherlands.

0305-4470/97/010129+13$19.50

the total energy

$$E_0 = \frac{1}{2}\sum_n \dot{x}_n^2 + \frac{1}{2}\sum_{n\neq m}\frac{f_{nm}^2}{(x_n - x_m)^2} \tag{4}$$

and a third one given by

$$Q = \tfrac{1}{2}\sum_{n\neq m} f_{nm}^2.$$

After transformation into the centre-of-mass system (corresponding to an unfolding of the spectra to a constant density of states) P vanishes. Alternatively one can take into account the centre-of-mass velocity by replacing expression (4) for the total energy by

$$E = \frac{1}{2}\sum_n (\dot{x}_n - \langle\dot{x}_n\rangle)^2 + \frac{1}{2}\sum_{n\neq m}\frac{f_{nm}^2}{(x_n - x_m)^2} \tag{5}$$

where the bracket denotes a local average. In the following this expression for E will be used exclusively.

If higher powers of $\dot{x}_n$ and f_{nm} are considered, a large number of additional constants of motion exists [4]. In fact it could be shown that the Pechukas–Yukawa equation system is completely integrable [5]. Thus a microcanonical phase-space distribution $\rho \propto \prod_i \delta(C_i - c_{i0})$ should be more appropriate, where the c_{i0} are the initial values for the constants of motion. Nevertheless ansatz (2) proved to be successful to describe a number of statistical properties of the spectra of chaotic systems correctly. First, for the eigenenergy distribution function, random matrix results are recovered [2, 6]. But also velocity distributions [7], asymptotic curvature distributions [8, 9], and the repulsion behaviour at avoided crossings [10, 11] are explained. In all these works it showed up that in chaotic systems just one constant of motion, namely the total energy E, is sufficient to describe the phase-space density,

$$\rho \sim \exp(-\beta E). \tag{6}$$

Thus one ends exactly at the Boltzmann ansatz of classical mechanics. Integrating equation (6) over the variables x_n and f_{nm} one gets a Gaussian velocity distribution

$$P_{\mathrm{vel}}(\dot{x}_n) \sim \exp\left(-\frac{\beta}{2}\sum_n (\dot{x}_n - \langle\dot{x}_n\rangle)^2\right). \tag{7}$$

One sees immediately that β can be expressed in terms of the quadratically averaged centre-of-mass velocities,

$$\beta^{-1} = \langle\dot{x}_n^2\rangle - \langle\dot{x}_n\rangle^2. \tag{8}$$

Provided that equation (6) really holds, β is the only free parameter in the model. Instead of studying the distribution functions of the dynamical variables one can alternatively concentrate on eigenvalue velocity autocorrelation functions [12]

$$C(t) = \left\langle \frac{\partial E_n(\bar{t})}{\partial \bar{t}}\,\frac{\partial E_n(\bar{t}+t)}{\partial \bar{t}} \right\rangle \tag{9}$$

or related quantities such as correlation functions for matrix elements [13] or wavefunctions [14]. In equation (9) the average is alternatively over $\bar{t}$, over the energy, or over different disorder configurations. With the help of supersymmetry techniques a number of exact results could be obtained here. In the present context the work of Simons and Altshuler [15] is of special importance; they found Gaussian velocity distribution functions in disordered systems with the strength of the magnetic flux or an external potential as the level-dynamics

parameter. This can be considered as an independent support of ansatz (2). The universal spectral correlations break down at energy scales of $\hbar/T_{\min}$, where $T_{\min}$ is the period of the shortest periodic orbit. At these scales periodic orbit theory has to be applied. Here especially the work of Berry and Keating [16] has to be mentioned where velocity autocorrelation functions are calculated, again with the magnetic flux as the level-dynamics parameter.

It is the object of this paper to explore the range of validity of the Yukawa–Boltzmann ansatz (2) with the help of experimentally obtained spectra of microwave billiards where the level dynamics is induced by the change of one billiard length. The paper focuses on three aspects. In section 2 the connection between Pechukas–Yukawa and billiard level dynamics is studied. It is *a priori* not self evident that both dynamics are equivalent, as in the first case the Hamiltonian is time-dependent and in the latter case it is the boundary condition. The idea nearest at hand is to transform the time dependence from the boundary to the Hamiltonian by means of conformal mapping. This, however, results in a nonlinear time dependence suggesting that the Pechukas–Yukawa model is a good description of billiard level dynamics only in the first order of time [7]. In this paper it is shown by a simple application of Green's theorem that in fact there is a *complete* equivalence for the case that one billiard length serves as a level-dynamics parameter. Section 3 contains the main result of this paper. Here a quantitative generic relation between β^{-1}, the temperature of the eigenvalue gas, and elementary geometric properties of the billiard is established. This is obtained by a periodic orbit calculation sketched already in our earlier work [7]. It is essentially an application of ideas developed by Berry in his work on the spectral rigidity [17] (similar techniques have been applied independently in [16, 18]). To the best of our knowledge this is the first example where β^{-1}, being usually considered as a free parameter, has been fixed by system properties. This allows very thorough tests of the Yukawa conjecture as now there is no free parameter left for adjusting the theory to the data. In section 4 these ideas are tested with experimental results from a series of microwave Sinai billiards of varying length. We studied the distributions of velocity, asymptotic curvature and closed approach distance at avoided crossings, but also $f_{n,n-1}$ distributions which have not been considered hitherto in the literature. In all cases a complete quantitative agreement with the expected behaviour was found, apart from some small deviations caused by the dominating bouncing-ball orbit.

2. On the equivalence of Pechukas–Yukawa and billiard level dynamics

To derive a relation between the change of a billiard shape and its level dynamics we start with a billiard with arbitrary area A and boundary S. Its eigenvalues x_n and eigenfunctions Ψ_n obey the Schrödinger equation

$$-\Delta\Psi_n = x_n\Psi_n \tag{10}$$

with the Dirichlet boundary condition $\Psi_{n|S} = 0$. After distortion of the billiard to a new area A_1 and a new boundary S_1 eigenvalues and eigenfunctions change to x_n^1 and Ψ_n^1, respectively, where now the Ψ_n^1 obey the Dirichlet boundary condition on S_1. The distortion may be arbitrary with the only restriction that the old billard is completely covered by the new one (it is always possible to obey this condition, if necessary after a proper blow-up of the distorted billiard). Application of Green's theorem now yields

$$(x_n^1 - x_m)\int_A \Psi_n^1\Psi_m \,\mathrm{d}A = \int_S \Psi_n^1(\nabla_\perp\Psi_m)\,\mathrm{d}s \tag{11}$$

where $\nabla_\perp$ denotes the normal derivative, directed outwards. For the sake of simplicity we assume for the moment that only one straight part L of the billiard is shifted whereas the remaining part of the boundary remains fixed (this is exactly the situation encountered in the experiment). Assuming without loss of generality that prior to the shift the movable wall coincides with the y-axis, and that a shift of Δl is performed in the direction of the positive x-axis, the right-hand side of equation (11) reads

$$\int_L \Psi_n^1(0, y)\frac{\partial \Psi_m(0, y)}{\partial x}\,\mathrm{d}y.$$

$\Psi_n^1(x, y)$ obeys the boundary condition $\Psi_n^1(\Delta l, y) = 0$. Expanding

$$\begin{aligned}\Psi_n^1(0, y) &= \Psi_n^1(\Delta l, y) - \Delta l\frac{\partial \Psi_n^1(\Delta l, y)}{\partial x} + \mathrm{O}((\Delta l)^2)\\ &= -\Delta l\frac{\partial \Psi_n(0, y)}{\partial x} + \mathrm{O}((\Delta l)^2)\end{aligned}$$

and performing the limit $\Delta l \to 0$ in equation (11), we find

$$\dot{x}_n = V_{nn} \tag{12}$$

for $n = m$, and

$$(x_n - x_m)\int \dot{\Psi}_n \Psi_m\,\mathrm{d}A = V_{nm} \tag{13}$$

for $n \neq m$. Here the dot means differentiation with respect to l, and V_{nm} is given by

$$V_{nm} = -\int_L \frac{\partial \Psi_n(0, y)}{\partial x}\frac{\partial \Psi_m(0, y)}{\partial x}\,\mathrm{d}y. \tag{14}$$

It is easy to show that for the general case the latter expression has to be replaced by

$$V_{nm} = -\int_S (\nabla_\perp \Psi_n)(\nabla_\perp \Psi_m) f(s)\,\mathrm{d}s \tag{15}$$

where $f(s)$ is a function depending on the details of the shape variation. If none of the walls moves inwards as was assumed in the beginning of this section then $f(s) \geqslant 0$ holds everywhere. Equation (12) shows that for this case all eigenvalue velocities are negative. For the *averaged* velocities this follows immediately from Weyl's law, for the *individual* velocities, however, it is by no means self-evident. An experimental demonstration of this fact can be found, for example, in figure 1 of [7].

To obtain an equation of motion for the V_{nm}, equation (15) is differentiated,

$$\dot{V}_{nm} = -\int_S \{(\nabla_\perp \dot{\Psi}_n)(\nabla_\perp \Psi_m) + (\nabla_\perp \Psi_n)(\nabla_\perp \dot{\Psi}_m)\} f(s)\,\mathrm{d}s - \int_S (\nabla_\perp \Psi_n)(\nabla_\perp \Psi_m)\dot{f}(s)\,\mathrm{d}s. \tag{16}$$

If $f(s)$ is constant in time, the second term on the right-hand side vanishes. This holds for the special case discussed above, where only one billiard wall is moved, and where one length is taken as the level-dynamics parameter. The first term can be transformed by applying the completeness relation to $\dot{\Psi}_n$,

$$\begin{aligned}\dot{\Psi}_n &= \sum_l \left(\int \dot{\Psi}_n \Psi_l\,\mathrm{d}A\right)\Psi_l\\ &= \sum_{l\neq n} \frac{V_{nl}}{x_n - x_l}\Psi_l\end{aligned} \tag{17}$$

where in the second step, equation (13) was used. Inserting expression (17) into equation (16), one ends with

$$\dot{V}_{nn} = 2\sum_{l\neq n}(V_{nl})^2\frac{1}{x_n - x_l} \tag{18}$$

for $n = m$ and

$$\dot{V}_{nm} = \sum_{l\neq n,m} V_{nl}V_{lm}\left(\frac{1}{x_n - x_l} + \frac{1}{x_m - x_l}\right) - V_{nm}\frac{V_{nn} - V_{mm}}{x_n - x_m} \tag{19}$$

for $n \neq m$. Equations (12), (18), and (19) are identical with the Pechukas–Yukawa equation system [1, 2]. This holds under the only restriction applied that the second term on the right-hand side of equation (16) vanishes.

As it was used in the derivation that the billiard area increases with time, the density of states is not constant. This can be corrected by introducing defolded variables $\bar{x}_n = Ax_n$ and $\bar{V}_{nm} = AV_{nm}$, respectively. The Pechukas–Yukawa equations for the new variables differ from the original ones by additional terms $(\dot{A}/A)\bar{x}_n$, $(\dot{A}/A)\bar{V}_{nn}$, and $(\dot{A}/A)\bar{V}_{nm}$ on the right-hand sides of equations (12), (18), and (19), respectively. As a consequence the total energy E (see equation (5)) is no longer a constant of motion but becomes proportional to the billiard area. In the light of the analogy between the eigenvalues of a chaotic system and a one-dimensional gas the increase of area corresponds to an adiabatic compression of the eigenvalue gas.

3. The Lagrange parameter β

The only parameter entering into the Yukawa conjecture (6) is the temperature $\beta^{-1} = \langle(\dot{x}_n)^2\rangle - (\langle\dot{x}_n\rangle)^2$. It cannot be considered as a *free* parameter, however: as the billiard boundary is the only quantity changed in the level dynamics, there must exist a relation between β^{-1} and geometrical properties of the billiard. To arrive at such a relation, we start with the periodic orbit expansion for the density of states $\rho(k) = \sum_m \delta(k - k_m)$, but with the wavenumber k as variable (which in the present context is more appropriate then the energy $x = k^2$) [19]:

$$\rho(k) = \frac{A}{2\pi}k + \sum_{p,n}\rho_{pn}l_p\cos\left(n\left(l_pk - \frac{\pi}{2}\nu_p\right)\right) \tag{20}$$

where A is the area of the billiard, l_p is the length of the primitive orbit p and ν_p its corresponding Maslov index. The second sum is over all primitive periodic orbits p and its repetitions n. As we are interested only in the asymptotic behaviour, only the leading term was taken for the smooth part $\rho_0(k)$ of $\rho(k)$. The prefactors ρ_{pn} are independent of k for isolated orbits and can be expressed in terms of the monodromy matrix describing the stability of orbit p. For the discussion of non-isolated orbits see e.g. [20].

Integration of equation (20) over k and subsequent differentiation with respect to the level-dynamics parameter t yields

$$\sum_m \dot{k}_m\delta(k - k_m) = -\frac{\dot{A}}{4\pi}k^2 - k\sum_{p,n}\rho_{pn}\dot{l}_p\cos\left(n\left(l_pk - \frac{\pi}{2}\nu_p\right)\right) \tag{21}$$

where it was assumed that the t dependence of the stability factor ρ_{pn} is only weak and can be neglected compared to that of l_p. Combining equations (20) and (21) one obtains

an expression for the velocity-weighted density of states

$$\rho_v(k) = \sum_m (\dot{x}_m - \langle \dot{x}_m \rangle)\delta(k - k_m)$$
$$= -2k^2\sqrt{A}\sum_{p,n}\rho_{pn}\frac{\mathrm{d}(l_p/\sqrt{A})}{\mathrm{d}t}\cos\left(n\left(l_p k - \frac{\pi}{2}\nu_p\right)\right) \tag{22}$$

where $\langle \dot{x}_n \rangle = -\dot{A}/A\langle x_n \rangle$ is the local centre-of-mass velocity. For the further procedure it is necessary to apply a Gaussian smearing of the delta functions,

$$\delta(\epsilon, k) = \frac{1}{\sqrt{\pi}\epsilon}\exp\left(-\left(\frac{k}{\epsilon}\right)^2\right). \tag{23}$$

The resulting expressions for the smeared densities of states $\rho(\epsilon, k)$ and $\rho_v(\epsilon, k)$ differ from equations (20) and (22) by an additional factor $\exp(-(\epsilon l_p/2)^2)$ on the right-hand sides ensuring convergence of the sums.

If ϵ is small compared to the mean distance between eigenvalues in the k-region in question, one obtains for the squared density of states

$$\rho^2(\epsilon, k) = \sum_n (\delta(\epsilon, k - k_n))^2 = \frac{1}{\sqrt{2\pi}\epsilon}\rho\left(\frac{\epsilon}{\sqrt{2}}, k\right) \tag{24}$$

and

$$\rho_v^2(\epsilon, k) = \frac{1}{\sqrt{2\pi}\epsilon}(\langle(\dot{x}_n)^2\rangle - (\langle \dot{x}_n \rangle)^2)\rho\left(\frac{\epsilon}{\sqrt{2}}, k\right). \tag{25}$$

Multiplying equations (24) and (25) by $\sqrt{2\pi}\epsilon$, inserting on the left-hand side the periodic orbit expansions for the densities of states, and performing the limit $\epsilon \to 0$ and a local average over k, one finds

$$\rho_0(k) = \lim_{\epsilon\to 0}\sqrt{2\pi}\epsilon\left\langle\left\{\sum_{p,n}\rho_{pn}l_p\cos\left[n\left(l_p k - \frac{\pi}{2}\nu_p\right)\right]\exp\left(-\left(\frac{\epsilon l_p}{2}\right)^2\right)\right\}^2\right\rangle \tag{26}$$

and

$$(\langle(\dot{x}_n)^2\rangle - (\langle \dot{x}_n \rangle)^2)\rho_0(k) = 4\langle x_n \rangle^2 A$$
$$\times \lim_{\epsilon\to 0}\sqrt{2\pi}\epsilon\left\langle\left\{\sum_{p,n}\rho_{pn}\frac{\mathrm{d}(l_p/\sqrt{A})}{\mathrm{d}t}\cos\left[n\left(l_p k - \frac{\pi}{2}\rho_p\right)\right]\exp\left(-\left(\frac{\epsilon l_p}{2}\right)^2\right)\right\}^2\right\rangle. \tag{27}$$

Equation (26) establishes a relation between the smooth part of the density of states and the oscillating one. A similar relation was already derived by Berry in his work on the spectral rigidity, but with a Lorentzian smearing of the deltafunctions [17]. The Gauss functions on the right-hand sides of equations (26) and (27) lead to a cut-off of the sums at lengths of the order of ϵ^{-1}. Thus in the limit $\epsilon \to 0$ the very long orbits give the dominating contributions to the sums on the right-hand sides of equations (26) and (27). One can therefore replace l_p and $\dot{l}_p$ by $N_p\langle l \rangle$ and $N_p\langle \dot{l} \rangle$, respectively, where N_p is the number of segments making up the orbit, and $\langle l \rangle$ is the average length of a segment. These averages differ from orbit to orbit, but the deviations from the global average over all orbits decrease with $N_p^{-1/2}$ (assuming that the very long orbits are distributed uniformly in phase space).

Dividing equation (27) by equation (26), the lattice sums cancel out, and one is left with

$$\langle \dot{x}_n^2 \rangle - \langle \dot{x}_n \rangle^2 = \left(2\frac{\langle \dot{l} \rangle}{\langle l \rangle} - \frac{\dot{A}}{A} \right)^2 \langle x_n \rangle^2. \tag{28}$$

As the step from equations (26) and (27) to equation (28) is crucial, two remarks may be appropriate [21]. First, it is *not* possible to argue from the exponential increase of the number of periodic orbits with length that the long orbits dominate the sums. This increase is cancelled by a corresponding decrease of the weight factors, as is discussed in [18]. Second, it is *not* necessary to apply the diagonal approximation to the double sums. Therefore the restriction of ϵ to values larger than the reciprocal Heisenberg time can be dropped [17, 18]. The result can still be further simplified by using that in ergodic billiards for every sufficiently long orbit the average segment length $\langle l \rangle$ is given by [22]

$$\langle l \rangle = \pi \frac{A}{S} \tag{29}$$

where A is the billiard area and S its circumference. This relation holds also for non-ergodic billiards, but here no self-averaging takes place, and one has to average over all orbits to get the correct result. One ends thus at

$$\sqrt{\langle \dot{x}_n^2 \rangle - \langle \dot{x}_n \rangle^2} = \beta^{-1/2} = \left| \frac{\dot{A}}{A} - 2\frac{\dot{S}}{S} \right| \langle x_n \rangle \tag{30}$$

expressing the quadratically averaged velocity in terms of billiard area and circumference alone. Equation (30) shows further that this average increases linearly with $\langle x_n \rangle$. To make the level dynamic homogeneous it is thus necessary to introduce rescaled variables $\hat{\dot{x}}_n = \dot{x}_n / \langle x_n \rangle$, $\hat{f}_{nm} = f_{nm} / \langle x_n \rangle$ etc. For the new variables the Yukawa relation reads

$$\rho \propto \exp(-\hat{\beta}\hat{E}) \tag{31}$$

where

$$\hat{\beta}^{-1} = \frac{\langle \dot{x}_n^2 \rangle - \langle \dot{x}_n \rangle^2}{\langle x_n \rangle^2} = \left| \frac{\dot{A}}{A} - 2\frac{\dot{S}}{S} \right|^2 \tag{32}$$

and where $\hat{E}$ is obtained from equation (5) by replacing all variables by the corresponding rescaled ones. Equations (31) and (32) are used in the next section for the comparison of the experimental results with the theoretical predictions.

The final results no longer contain any ingredients from periodic orbit theory because of the complete cancellation of the sums in equations (26) and (27). One may suspect that a more direct way to arrive at equation (32) exists without making use of periodic orbit theory. A possible starting point is equation (15) from which one obtains, for the quadratically averaged velocities,

$$\langle (\dot{x}_n)^2 \rangle = \int_S \int_{S'} \langle [\nabla_\perp \Psi_n(s) \nabla_\perp \Psi_n(s')]^2 \rangle f(s) f(s') \, \mathrm{d}s \, \mathrm{d}s' \tag{33}$$

where the bracket again denotes a local average. Recently similar averages have been calculated in disordered systems [23, 24]. We have not been able, however, to derive equation (32) in this way.

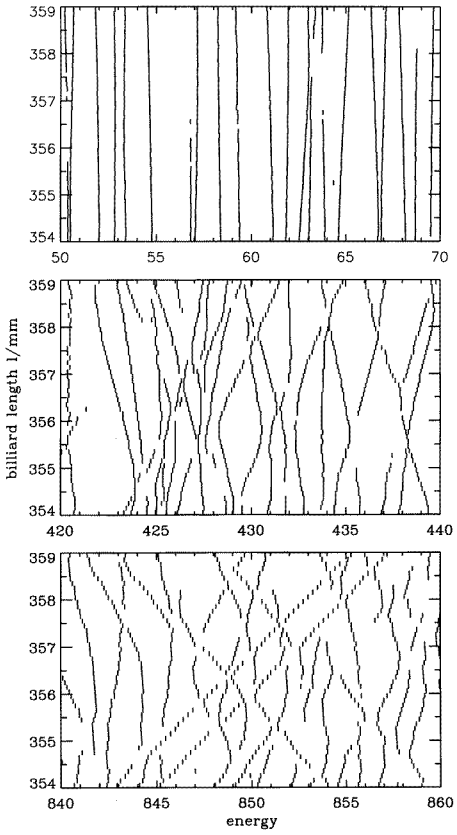

Figure 1. Spectra of the quartered Sinai billiards with $a = 354 \ldots 359$ mm, $b = 237$ mm, $r = 70$ mm in three different energy regions. The spectra were unfolded to a constant density of states of 1 using the Weyl formula (see equation (34)).

4. Experimental tests of the Yukawa conjecture

In the preceeding section we succeeded in establishing a relation between the Lagrange parameter $\hat{\beta}$ and elementary geometric billiard properties. This allows tests of the Yukawa conjecture (31) with no adjustable parameter left in the model. To this end we measured the spectra of a number of microwave billiards shaped as quartered Sinai billiards with fixed short side b, fixed radius of the quarter circle r, and varying long side a taking the role of the time. To get an impression of the observed level dynamics, figure 1 shows typical spectra in three different energy ranges. All spectra were unfolded to a mean density of states of one using the leading terms of the Weyl formula

$$\rho_{\mathrm{Weyl}}(x) = \frac{A}{4\pi} - \frac{S}{4\pi\sqrt{x}} \tag{34}$$

which corresponds to a transformation into the centre-of-mass velocity.

The figure clearly exhibits the increasing violence of the level dynamics with energy. It illustrates also the limitations of the experimental approach. Eigenvalues eventually disappear and reappear again while changing the length. This happens whenever a node line passes the position of the coupling antenna. Furthermore, eigenvalues are lost close to avoided crossings as soon as the distance becomes smaller than the experimental resolution of some MHz. If the missing levels are completed, the resulting integrated density of states agrees up to about 0.5% with the values obtained from the Weyl formula (34). As it is not possible, however, to reconstruct the exact positions of the missing levels, only the resonances really seen in the experiment are considered in the following.

The distributions and histograms to be presented now are obtained from spectra of quartered Sinai billiards with $r = 70$ mm, $b = 200$ mm, and a varying between 460 and 480 mm. The applied step width varied with frequency and was 1 mm between 0 and 8 GHz, 0.5 mm between 8 and 12 GHz and 0.2 mm between 12 and 15 GHz. Altogether some 600 eigenvalues were registered in an individual spectrum amounting to a total of about 12 000 eigenvalues considered. For the corresponding Lagrange parameter one gets from equation (32)

$$\begin{aligned}\hat{\beta} &= \left|\frac{\dot{A}}{A} - 2\frac{\dot{S}}{S}\right|^{-2} \\ &= \left|\frac{b}{ab - \frac{\pi}{4}r^2} - \frac{4}{2a + 2b - (2 - \frac{\pi}{2})r}\right|^{-2} \\ &= 1.434m^2 \end{aligned} \tag{35}$$

where for a an average value of 470 mm was taken. Due to the change of a, $\hat{\beta}$ varies by $\pm 2\%$ about its average value. In the analysis of the data two alternatives were pursued. First, for all distributions to be discussed below the theoretical curves were calculated taking $\hat{\beta}$ from equation (35). The resulting curves are shown in figures 2–6 as full curves. Then the theoretical curves were fitted to the data considering $\hat{\beta}$ as a free parameter. The corresponding curves are shown as broken curves in the figures, and the resulting $\hat{\beta}$ values, including their standard deviations, are compiled in table 1.

Figure 2 shows the eigenvalue velocities, averaged quadratically over 20 neighbouring eigenvalues, as a function of energy. One observes the linear increase predicted by equation (30) but superimposed by oscillations which are caused by the bouncing-ball orbit parallel to the short side of the billiard (for more details see [7, 25]). For the slope of the linear increase a value of $\hat{\beta}^{-1/2} = 0.835$ m^{-1} is expected. The straight line shown in figure 2 corresponds to this theoretical prediction, the broken line has been obtained from the fit. A similar good agreement between experiment and theory was obtained for the level-dynamics measurements shown in figure 1.

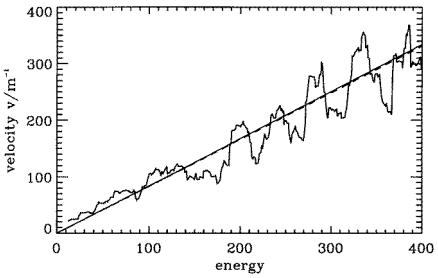

Figure 2. Eigenvalue velocities, quadratically averaged over 20 neighbours, in a quartered Sinai billiard (for geometrical dimensions see text). The slope of the straight full line corresponds to the theoretical prediction from equation (35), the broken line represents the best fit. The oscillations are due to the dominating bouncing-ball orbit.

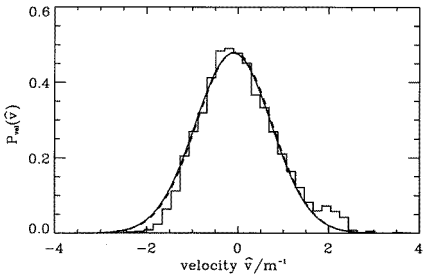

Figure 3. Distribution of the rescaled velocities. The full curve corresponds to the theoretical predictions from equation (36), the broken curve results from a fit. The deviations in the wings are caused by the bouncing ball parallel to the short side of the billiard. The regions with $|\hat{v}| > 1.5$ m^{-1} were omitted in the fit.

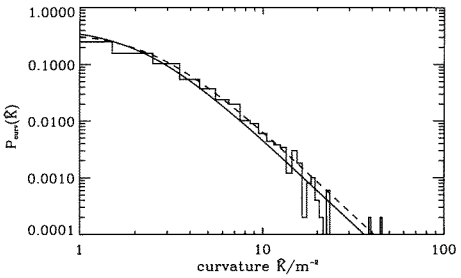

Figure 4. Distribution of the rescaled curvatures, theoretical prediction from equation (37) (full curve), and fit with $\hat{\beta}$ as a free parameter (broken curve).

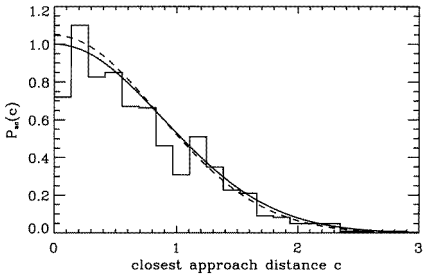

Figure 5. Distribution of the closest approach distances of neighboured eigenvalues at avoided crossings, the theoretical prediction from equation (38) (full curve), and a fit with the width as a free parameter (broken curve).

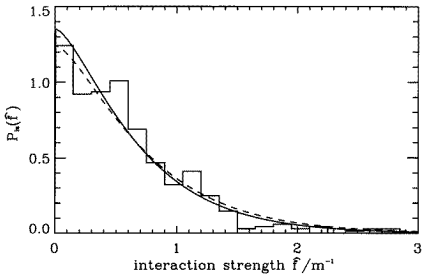

Figure 6. Distribution of the rescaled nearest-neighbour interaction strengths, theoretical prediction from equation (41) (full curve) and fit with $\hat{\beta}$ as a free parameter (broken curve).

Table 1. Values for $\hat{\beta}$, corresponding to the reciprocal temperature of the eigenvalue gas, as obtained from theory and from fits to the different experimental distribution functions. The given errors correspond to one standard deviation. In the case of the theoretical value the given error denotes the range passed by $\hat{\beta}$ in changing the billiard length from 460 to 480 mm.

	$\hat{\beta}$ m^{-2}
Theory (equation (35))	1.434(30)
Eigenvalue velocities (equation (30) and figure 2)	1.46(6)
Velocities distribution (equation (36) and figure 3)	1.45(3)
Curvature distribution (equation (37) and figure 4)	1.29(41)
Interaction-strength distribution (equation (41) and figure 6)	1.21(39)

Now we investigate the velocity distribution $P_{\mathrm{vel}}(\hat{v})$. Here the Yukawa conjecture predicts a Gaussian distribution

$$P_{\mathrm{vel}}(\hat{v}) = \sqrt{\frac{\hat{\beta}}{2\pi}}\,\exp\left(-\frac{\hat{\beta}}{2}\hat{v}^2\right). \tag{36}$$

Figure 3 shows the histogram of the experimental velocity distribution, together with the prediction (36), using the same value for $\hat{\beta}$ as above. Again excellent agreement is found between the theoretical prediction and the fit with $\hat{\beta}$ considered as a free parameter. The small but significant deviations in the wings are caused by the already mentioned bouncing-ball orbit. If the energy regions disturbed by the bouncing ball orbit are omitted from the histogram, the shoulder on the high velocity side disappears. Similar deviations can be found allready in our earlier work [7], as well as in a recent publication by Sieber *et al* [25].

The quantity most thoroughly studied in level dynamics is the distribution $P_{\text{curv}}(\hat{K})$ of curvatures $\hat{K}_n = \ddot{x}_n/\langle x_n\rangle^2$. Starting from the Yukawa conjecture (31), Gaspard *et al* [8] showed that for GOE systems $P_{\text{curv}}(\hat{K})$ decreases asymptotically with $|\hat{K}|^{-3}$. Zakrzewski and Delande [9] found from numerical studies that $P_{\text{curv}}(\hat{K})$ is described for all $\hat{K}$ accurately by

$$P_{\text{curv}}(\hat{K}) = \frac{\hat{\beta}}{2\pi}\left(1 + \left(\frac{\hat{\beta}\hat{K}}{\pi}\right)^2\right)^{-3/2}. \tag{37}$$

Recently it was proven by v Oppen [26], using supersymmetry techniques, that equation (37) indeed is the correct curvature distribution. Figure 4 shows the corresponding experimental result. The agreement between theory and experiment is again good. We were not able to see deviations from equation (37) caused by the bouncing ball as they are reported, for example, for the stadium billiard [27, 9] and the Sinai billiard [25]. These deviations should become manifest mainly in the region of small curvatures where the precision of our data was not sufficient to allow a reliable determination of the curvatures.

Now we come to the discussion of avoided crossings. Zakrzewski and Kuś [10] showed that for the GOE the closest approach distances c of neighboured eigenvalues at avoided crossings should be Gaussian distributed,

$$P_{ac}(c) = \exp\left(-\frac{c^2}{\pi}\right). \tag{38}$$

In a more recent work the authors published an improved expression for $P_{ac}(c)$ [11] which yielded, however, only marginal modifications; therefore, the much simpler expression (38) is used here. Contrary to the distributions considered up to now $\hat{\beta}$ does not enter at all here. The distribution of closest approach distances is thus universal, as soon as the mean eigenvalue spacing is normalized to one. The full curve in figure 5 again demonstrates the good agreement between experiment and theory. The small hole in the lowest histogram bar is caused by the experimental loss at closely neighboured eigenresonances. Again an additional fit was performed by allowing for an additional factor a in the exponent (and a prefactor $\sqrt{a}$ for normalization). The fit yielded $a = 1.1(1)$ thus confirming again the theory quantitatively.

For a last test of the Yukawa conjecture we return to the dynamic-equation system (12), (18), and (19). Near close encounters of neighbouring eigenvalues x_{n-1} and x_n the dynamics can be approximated by a two-body collision, and equations (12) and (18) simplify to

$$\ddot{x}_n = -\ddot{x}_{n-1} = 2\frac{|f_{n,n-1}|^2}{|x_n - x_{n-1}|^3}. \tag{39}$$

As positions and accelerations are known from the experiment, equation (39) can be used to extract the nearest-neighbour interaction strengths $f_{n,n-1}$. For the distribution $P_{\text{is}}(\hat{f})$ of the rescaled nearest-neighbour interaction strengths the Yukawa conjecture yields

$$P_{\text{is}}(\hat{f}) = N\int \exp\left(-\hat{\beta}\frac{\hat{f}^2}{x^2}\right)P(x)\,\mathrm{d}x \tag{40}$$

where N is a normalization constant and $P(x)$ is the nearest-neighbour spacing distribution. Inserting for $P(x)$ the Wigner surmise

$$P(x) = \frac{\pi}{2}x\exp\left(-\frac{\pi}{4}x^2\right)$$

the integration can be carried out and yields

$$P_{\text{is}}(\hat{f}) = 2\hat{\beta}\hat{f}K_1\left(\sqrt{\pi\hat{\beta}}\hat{f}\right) \tag{41}$$

where $K_1(x)$ is a modified Bessel function.

In the experimental determination of the $f_{n,n-1}$ we face a problem. For the two-body-collision approximation to be justified the interaction with the other eigenvalues, especially x_{n-2} and x_{n+1}, has to be small. This suggests that we consider $f_{n,n-1}$ values only if the relation

$$|x_{n-1} - x_{n-2}|^{-3} + |x_{n+1} - x_n|^{-3} < q|x_n - x_{n-1}|^{-3}$$

holds, where q is a cut-off parameter which has to be properly adjusted. On one hand q has to be small for the two-body-collision approximation to be justified, on the other hand it has to be large for obtaining a representative ensemble of nearest-neigbour spacings. Fortunately a variation of q showed only little influence on the resulting distribution for q values between 0.2 and 0.9. Figure 6 shows the histogram for the rescaled interaction strengths $\hat{f}_{n,n-1}$ for $q = 0.5$ together with the theoretical curve obtained from equation (41). We would like to point especially at the exponential and definitely non-Gaussian decrease of the distribution for large $\hat{f}_{n,n-1}$ values.

5. Summary

From figures 2–6 and table 1 we see that in all cases the $\hat{\beta}$ values obtained from the fit as well as the width of the distribution of closest approach distances are in quantitative agreement with the theoretical predictions. This shows that the Boltzmann ansatz can account perfectly well for all found distributions, apart from small deviations due to non-generic features such as bouncing-ball orbits. We would like to stress, that the only parameter $\hat{\beta}$, corresponding to the reciprocal temperature of the eigenvalue gas, was determined independently from the billiard geometry. So to speak the Boltzman ansatz has been tested in this work even more profoundly than it would be possible in ordinary statistical mechanics, as positions, velocities, acceleration etc of all particles are known at every moment which obviously is out of reach for an ordinary gas.

Acknowledgments

We gratefully acknowledge fruitful discussions with B Eckhardt, Oldenburg at various stages of the experimental work and the manuscript. The experiments profited much from the existing software for data aquisition and analysis written by J Stein. The work was supported by the Deutsche Forschungsgemeinschaft via the Sonderforschungsbereich ‘Nichtlineare Dynamik’.

References

[1] Pechukas P 1983 *Phys. Rev. Lett.* **51** 943
[2] Yukawa T 1985 *Phys. Rev. Lett.* **54** 1883
[3] Hasegawa H and Robnik M 1993 *Europhys. Lett.* **23** 171
[4] Yukawa T 1986 *Phys. Lett.* **116A** 227
[5] Nakamura K and Lakshmanan M 1986 *Phys. Rev. Lett.* **57** 1661
[6] Haake F 1991 *Quantum Signature of Chaos* (Heidelberg: Springer)
[7] Kollmann M, Stein J, Stoffregen U, Stöckmann H-J and Eckhardt B 1994 *Phys. Rev.* E **49** R1
[8] Gaspard P, Rice S A, Mikeska H J and Nakamura K 1990 *Phys. Rev.* A **42** 4015
[9] Zakrzewski J and Delande D 1993 *Phys. Rev.* E **47** 1650
[10] Zakrzewski J and Kuś M 1991 *Phys. Rev. Lett.* **67** 2749
[11] Zakrzewski J, Delande D and Kuś M 1993 *Phys. Rev.* E **47** 1665

[12] Szafer A and Altshuler B L 1993 *Phys. Rev. Lett.* **70** 587
[13] Taniguchi N, Andreev A V and Altshuler B L 1995 *Europhys. Lett.* **29** 515
[14] Mucciolo E R, Simons B D, Andreev A V and Prigodin V N 1995 *Phys. Rev. Lett.* **75** 1360
[15] Simons B D and Altshuler B L 1993 *Phys. Rev.* B **48** 5422
[16] Berry M V and Keating J P 1994 *J. Phys. A: Math. Gen.* **27** 6167
[17] Berry M V 1985 *Proc. R. Soc.* A **400** 229
[18] Eckhardt B, Fishman S, Keating J, Agam O, Main J and Müller K 1995 *Phys. Rev.* E **52** 5893
[19] Gutzwiller M 1990 *Chaos in Classical and Quantum Mechanics* (New York: Springer)
[20] Sieber M, Smilansky U, Creagh S C and Littlejohn R G 1993 *J. Phys. A: Math. Gen.* **26** 6217
[21] Eckhardt B Private communication
[22] Koga S 1995 *Prog. Theor. Phys.* **93** 19
[23] Prigodin V N 1995 *Phys. Rev. Lett.* **74** 1566
[24] Fyodorov Y V and Mirlin A D 1995 *Phys. Rev.* B **51** 13 403
[25] Sieber M, Primack H, Smilansky U, Ussishkin I and Schanz H 1995 *J. Phys. A: Math. Gen.* **28** 5041
[26] v Oppen F 1995 *Phys. Rev.* E **51** 2647
[27] Takami T and Hasegawa H 1992 *Phys. Rev. Lett.* **68** 419